



Słodczyk, E., Pietranik, A., Glynn, S., Wiedenbeck, M., Breitzkreuz, C., & Dhuime, B. (2018). Contrasting sources of Late Paleozoic rhyolite magma in the Polish Lowlands: evidence from U–Pb ages and Hf and O isotope composition in zircon. *International Journal of Earth Sciences*, 1-17. <https://doi.org/10.1007/s00531-018-1588-8>

Publisher's PDF, also known as Version of record

License (if available):
CC BY

Link to published version (if available):
[10.1007/s00531-018-1588-8](https://doi.org/10.1007/s00531-018-1588-8)

[Link to publication record in Explore Bristol Research](#)
PDF-document

This is the final published version of the article (version of record). It first appeared online via SPRINGER at <https://link.springer.com/article/10.1007%2Fs00531-018-1588-8> . Please refer to any applicable terms of use of the publisher.

University of Bristol - Explore Bristol Research

General rights

This document is made available in accordance with publisher policies. Please cite only the published version using the reference above. Full terms of use are available:
<http://www.bristol.ac.uk/red/research-policy/pure/user-guides/ebr-terms/>



Contrasting sources of Late Paleozoic rhyolite magma in the Polish Lowlands: evidence from U–Pb ages and Hf and O isotope composition in zircon

Elżbieta Słodczyk¹ · Anna Pietranik¹ · Sarah Glynn^{2,3} · Michael Wiedenbeck³ · Christoph Breitkreuz⁴ · Bruno Dhuime⁵

Received: 7 September 2016 / Accepted: 28 January 2018
© The Author(s) 2018. This article is an open access publication

Abstract

The Polish Lowlands, located southwest of the Teisseyre–Tornquist Zone, within Trans-European Suture Zone, were affected by bimodal, but dominantly rhyolitic, magmatism during the Late Paleozoic. Thanks to the inherited zircon they contain, these rhyolitic rocks provide a direct source of information about the pre-Permian rocks underlying the Polish Lowland. This paper presents zircon U–Pb geochronology and Hf and O isotopic results from five drill core samples representing four rhyolites and one granite. Based on the ratio of inherited vs. autocrystic zircon, the rhyolites can be divided into two groups: northern rhyolites, where autocrystic zircon is more abundant and southern rhyolites, where inherited zircon dominates. We suggest that the magma sources and the processes responsible for generating high silica magmas differ between the northern and southern rhyolites. Isotopically distinct sources were available during formation of northern rhyolites, as the Hf and O isotopes in magmatic zircon differ between the two analysed localities of northern rhyolites. A mixing between magmas formed from Baltica-derived mudstone–siltstone sediments and Avalonian basement or mantle can explain the diversity between the zircon compositions from the northern localities Daszewo and Wysoka Kamieńska. Conversely, the southern rhyolites from our two localities contain zircon with similar compositions, and these units can be further correlated with results from the North East German Basin, suggesting uniform source rocks over this larger region. Based on the ages of inherited zircon and the isotopic composition of magmatic ones, we suggest that the dominant source of the southern rhyolites is Variscan foreland sediments mixed with Baltica/Avalonia-derived sediments.

Keywords Zircon isotopic composition · Rhyolite petrogenesis · Trans-European Suture Zone · Crustal basement diversity

Electronic supplementary material The online version of this article (<https://doi.org/10.1007/s00531-018-1588-8>) contains supplementary material, which is available to authorized users.

✉ Elżbieta Słodczyk
elzbieta.slodczyk@uwr.edu.pl

¹ Institute of Geological Sciences, University of Wrocław, ul. Cybulskiego 30, 50-205 Wrocław, Poland

² School of Geosciences, University of the Witwatersrand, Witwatersrand, South Africa

³ Deutsches GeoForschungsZentrum GFZ, Potsdam, Germany

⁴ Institute for Geology and Palaeontology, TU Bergakademie Freiberg, Bernhard-von-Cotta-Str. 2, Freiberg, Germany

⁵ University of Bristol, Bristol, UK

Introduction

The Central European Basin was affected by extensive magmatism with the emplacement of c. 80,000 km³ of magma during the Late Carboniferous to Early Permian (Paulick and Breitkreuz 2005). This resulted in a bimodal volcanism which is observed across central Europe (Benek et al. 1996; Breitkreuz and Kennedy 1999; Geißler et al. 2008; Hoffmann et al. 2012; Kryza and Awdankiewicz 2012; Awdankiewicz et al. 2013; Turniak et al. 2014; Fig. 1a). In Poland, volcanism extended from the Fore-Sudetic Monocline northwards up to Western Pomerania. The resulting Permo-Carboniferous volcanic rocks are today covered by younger sediments with thickness varying from approximately 1000 m in the Fore-Sudetic Monocline to over 5000 m close to the Teisseyre–Tornquist Zone (TTZ; Fig. 1); (Jackowicz 1994; Maliszewska et al. 2003; Dadlez 2006). Hence, in Poland, samples of such volcanic rocks are provided exclusively

Fig. 1 **a** Plate tectonic sketch of West and Central Europe after Smit et al. 2016; *TTZ* Teisseyre–Tornquist Zone, *L* Laurentia; **b** map of northwestern Poland indicating the location of the sampling sites of Permo-Carboniferous volcanic rocks. Numbers indicate the thickness of drilled volcanic rocks in meters (data from Dadlez 2006; Geißler et al. 2008). Map modified after Dadlez (2006), and Breitzkreuz et al. (2007). Teisseyre–Tornquist Zone based on compilation map from Grad and Polkowski (2016)



from drill cores obtained during an intense hydrocarbon exploration program carried out from the 1970s through until the 1990s. The volcanic rocks constitute less than 12% of the material in the drill cores (Breitzkreuz et al. 2007), but in many places, they provide crucial information about

the underlying pre-Permian basement. The composition of the pre-Permian basement is also constrained by geophysical studies (Grad et al. 2003; Dadlez et al. 2005; Guterch and Grad 2010) and drill core data showing the presence of Ordovician-to-Carboniferous sediments (Podhalańska

and Modliński 2006; Matyja 2006). The pre-Permian basement is probably composed of several Precambrian-to-lower Paleozoic units that have been interpreted as having formed through a juxtaposition of several fragments of continental crust along the margin of Baltica prior to being overlain by sedimentary and low-grade metasedimentary cover (Mazur et al. 2010, 2015; Żelaźniewicz et al. 2016).

An interpretation whereby some of the underlying crust may be composed of Baltica-derived sediments is supported by recent studies on detrital and inherited zircons of the North East German Basin (NE GB; Pietranik et al. 2013a) and of the Mid-German Crystalline Rise in central Germany (Zeh and Gerdes 2010). It is, therefore, reasonable to expect that data from zircons from volcanic rocks from the Polish Lowlands will provide additional constraints on crustal structures and their arrangement during the Late Paleozoic.

Here, we present new analyses of zircon from four rhyolitic (boreholes Daszewo, Wysoka Kamieńska, Chrzypsko, and Pniewy) and one granitic (borehole Chrzypsko; Fig. 1b) units. Our data include Secondary Ion Mass Spectrometry (SIMS) U–Pb ages and O isotope analyses followed by Hf isotope analyses using Laser Ablation Inductively Coupled Mass Spectrometry (LA–ICP–MS). The goal of the present contribution is to constrain the sources of rhyolite magma in the Polish Lowlands and to fit this information into current models of continental crust and plate tectonic evolution in the region (Mazur et al. 2015; Smit et al. 2016; Żelaźniewicz et al. 2016). In addition, we address the extent to which rhyolite magmas were the product of remelted crustal granitic bodies.

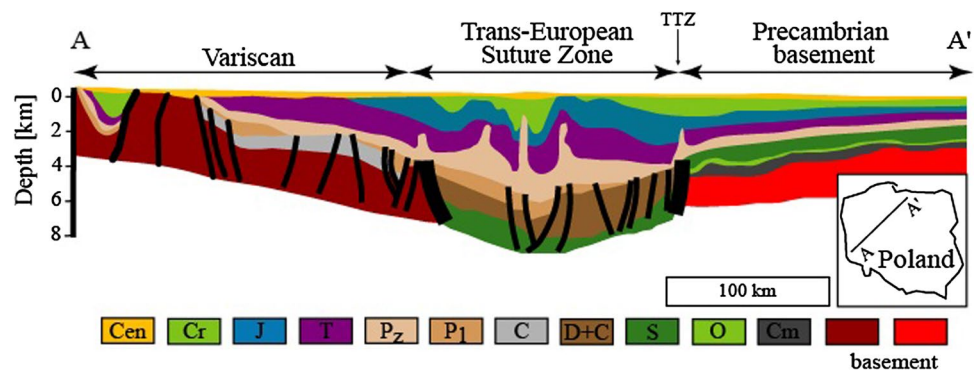
Geological setting

The investigated zircons were extracted from: (1) drill cores of rhyolitic lavas and ignimbrites in the western part of the Polish Lowlands and (2) a granite underlying Permian volcanics near Poznań city. All our samples lie within the Polish Basin, in the easternmost part of the Southern Permian Basin, which is part of the central European

Permo-Mesozoic basin system (Kiersnowski et al. 1995; VanWees et al. 2000; Littke et al. 2005). The Polish Basin formed along the NW–SE trending TTZ, which constitutes the southwestern margin of the East European Platform (Fig. 1b; Dadlez et al. 2005). The TTZ is one of the most important crustal-scale boundaries in Europe (Zielhuis and Nolet 1994; Schweitzer 1995; Pharaoh 1999), and has been investigated in detail using high-quality, deep refraction seismics (Fig. 2; Grad et al. 2003, 2006, 2012; Guterch and Grad 2010). Mazur et al. (2016) have merged these results with potential field data. The filling of the Polish Basin has also been constrained by numerous boreholes, which show successions of variable thicknesses of Ordovician to Cenozoic deposits containing several unconformities (Jackowicz 1994; Protas et al. 1995; Maliszewska et al. 2003; Breitreuz et al. 2007; Modliński and Podhalańska 2010).

The volcanic rocks in drill cores are commonly Late Carboniferous to Early Permian in age (Breitreuz et al. 2007). Facies analysis has revealed the presence of lava flows and pyroclastic deposits (Jackowicz 1994; Breitreuz et al. 2007). These volcanics are best preserved in areas of subsidence, where the thickness of volcanic rocks can exceed 1550 m, commonly decreasing eastwards (Fig. 1b; Jackowicz 1994; Maliszewska et al. 2003; Dadlez 2006). In this study, samples were taken from drill cores in (1) Wysoka Kamieńska, a 480-m-thick porphyritic rhyolite lava flow with feldspar phenocrysts < 0.5 cm (down hole sampling depth: 3500 m); (2) a 230-m-thick, weakly porphyritic dacite/rhyolite lava flow in Daszewo (sampling depth: 3450 m); and (3) a 150-m-thick ignimbrite in Pniewy 3 (sampling depth: 3875 m; Breitreuz et al. 2007). The granite and one rhyolitic sample come from the Chrzypsko well (sampling depth: 4218 m), which comprises an upper sedimentary succession with 470 m of rhyolites and ignimbrites underlain by a granitic body with a minimum thickness of 254 m (Żelaźniewicz et al. 2016). The rhyolite drill core samples analysed in this study were previously dated by Breitreuz et al. (2007) using SHRIMP (sensitive high resolution ion micro-probe) and yielded concordant ages between 293.0 ± 1.2 and 298.5 ± 1.7 Ma (1 SD). The zircon separated

Fig. 2 Geological and seismic section through Poland across A–A' line marked in the inset (after Grad and Polkowski 2016); TTZ Teisseyre–Tornquist Zone



from the Chrzypsko granite gave a slightly older SHRIMP age of ca. 302 Ma (Żelaźniewicz et al. 2016).

Not much is known about the pre-Permian basement at the sampling sites, apart from seismic data from the Daszewo and the Pniewy/Chrzypsko regions and several boreholes that sampled Carboniferous and pre-Carboniferous sediments. In the northern part of the Polish Lowland rocks older than Carboniferous were drilled in several localities, particularly, noteworthy were drilling profiles from the Koszalin–Chojnice Zone (Ordovician–Silurian, Poprawa et al. 2006; Modliński and Podhalańska 2010). From the localities analysed in this study Daszewo is located in the Koszalin–Chojnice Zone (Dadlez et al. 2005), so the seismic and drilling data can provide information on the source of Daszewo rhyolites. Refraction seismic data reveal that within this segment the crust has three layers: an upper layer of consolidated crust from 11 to 20 km, a middle layer at depths between 20 and 26 km, and a lower layer at depths of 26–36 km (Dadlez 2006). The nature of the upper-most part of the crust is also constrained by electromagnetic data, which indicate that it is dominated by Paleozoic metasediments (Ernst et al. 2008; Jóźwiak 2013). This upper crust was penetrated by several boreholes and the deepest deposits were a clay to mudstone sequence of Ordovician age as well as Silurian shales and siltstones. This upper crust may also be composed of coal facies and products of crustal brines transported through fault systems (Ernst et al. 2008). The sedimentary cover within the investigated area is composed of lower Rotliegend volcanic and subordinate sedimentary rocks, which extends over the paleotopography of the top Carboniferous surface, including the covering of grabens, horsts and tilted fault blocks (Pożaryski et al. 1992; Dadlez 2006). The U–Pb ages of the detrital zircons supplied to the Koszalin Chojnice zone (boreholes Słupsk IG and Nowa Karczma 1) cluster at 1756–2050, 1485–1510, 974–1227, 739–805, 854–856, 559–623, and 442–495 Ma (Poprawa et al. 2006). These zircon come from clastics delivered to the Koszalin–Chojnice zone from variable sources such as basement elements that were detached from the margin of Baltica and from the Avalonia Terrane, subduction-related volcanic island arc rocks and sediments of the accretionary prism (see Nawrocki and Poprawa 2006; Poprawa 2006).

The Pniewy and Chrzypsko sampling sites are located within the Fore Sudetic Monocline, which deep refraction data reveal a typical crustal profile for the Trans European Suture Zone (TESZ): thick (12 km) units consisting of folded Early Paleozoic sediments, underlain by intermediary crystalline units with a thickness of ~5 km, and a lower crystalline crust (Dadlez 2006). These Carboniferous sediments were penetrated by the Września IG-1 borehole and include monotonous turbidities deposited after 320 Ma (Mazur et al. 2010). Geochemical and detrital zircon age data from these sediments point to either

a continental island arc or an active continental margin provenance for the precursor clastic materials (see Mazur et al. 2010). In addition, Early Paleozoic phyllites were drilled over the Wolsztyn–Leszno High (metamorphic age: 358.6 ± 1.8 Ma; see Mazur et al. 2006; protolith age: Early Paleozoic–Devonian; see Haydukiewicz et al. 1999). Mazur et al. (2010) studied zircons from Carboniferous turbidites that were located close to the Pniewy borehole, which contributes to this current study. They obtained the zircon ages in the ranges of 2081 ± 18 , 566 ± 10 , 544 ± 8 , 516 ± 6 , 426 ± 5 , 380 ± 5 Ma.

There is an ongoing debate about the crystalline basement under the central part of the European continent including the Polish Lowlands. Three different models have been proposed (see Mazur et al. 2015 for summary): (1) far East Avalonia is trapped between the East European Craton and the Variscan orogen; (2) the margin of the Teisseyre–Tornquist Zone is formed by the amalgamation of two lithospheric blocks that originated from Baltica and which had differing thicknesses; and (3) Baltica extended to the southwest from the Teisseyre–Tornquist Zone, forming an Early Paleozoic passive margin. This last scenario is supported by recent studies of Smit et al. (2016), who observed a 50–100-km-wide low P-wave velocity zone (see also Fig. 1a) forming a distinctive crustal domain between Avalonia and Baltica.

Analytical methods

Zircon grains were extracted from samples taken from the four drill cores Daszewo, Wysoka Kamieńska, Pniewy 3 and Chrzypsko (Fig. 1b). The first three samples consist of Permian rhyolites that were previously dated using U–Pb zircon method by Breitkreuz et al. (2007). The Chrzypsko drill core contains a rhyolite in unconformable contact with an underlying granite, both of which we investigated. Zircon grains were recovered from 4-cm diameter half-cores that had been carefully cleaned. All samples were without cracks and were ~3 kg in mass. Zircon grains were separated by standard crushing, panning and magnetic separation techniques. The five concentrates were prepared as two 25.4-mm diameter, round epoxy grain mounts in which the zircon grains were cast and then sectioned by polishing. Both the 91500 and Plešovice zircon reference materials (Wiedenbeck et al. 1995; Sláma et al. 2008) were also embedded in each mount. In order to identify zonation and other internal structures within the grains in advance of data acquisition, our mounts were investigated optically using a petrographic microscope as well as with BSE (Back Scattered Electron) images using a Jeol Hyperprobe JXA-8500F microprobe at the Helmholtz Zentrum Potsdam (GFZ; see Appendix 1 for images).

Major elemental determinations

Chemical analyses of the polished mounts were obtained using a Jeol Hyperprobe JXA-8500F in Potsdam with a wavelength-dispersive detector. An accelerating voltage of 20 kV was used in order to generate sufficiently intense signals for the required elements. The electron beam current was 20 nA and the probe diameter was 1 μm . The following calibrants were used: Zircon for Si ($K\alpha$) and Zr ($L\alpha$), Hf alloy for Hf ($L\beta$), ScPO_4 for Sc ($K\alpha$) and U alloy for U ($M\beta$). Our Hf alloy calibrant is 99.97% pure Hf and the U alloy is 99.7% pure U. The acquisition times were 30 s for Si and Zr and 40 s for Hf, Sc and U. The acquisition time to collect the background level on both sides of the corresponding peak was half of the peak acquisition time. Detection limits were 100 $\mu\text{g/g}$ for Si and Sc, 150 $\mu\text{g/g}$ for U, 300 $\mu\text{g/g}$ for Zr and 600 $\mu\text{g/g}$ for Hf. The Hf (LL) line has an intensity of 3% and can be neglected with regard to the high amount of Si detected.

To check the accuracy of the major element measurements, grains of Plešovice and 91500 were also analysed. Although isotopically homogenous, 91500 has been reported to have a range of Hf concentrations. For example, Gool-aerts et al. (2004) report values from 5610 to 6360 $\mu\text{g/g}$ for a single grain. This range was in agreement with the measurements done over the course of this session (average of 6297 $\mu\text{g/g}$). Similarly the Hf abundance values in Plešovice zircon also show large variations between 8000 and 14,000 $\mu\text{g/g}$, which is similar to the range of 9000 to 12,000 $\mu\text{g/g}$ reported by Schoene et al. (2010), and also in agreement with the Hf values of 8000–14,000 $\mu\text{g/g}$ reported by Sláma et al. (2008).

Secondary ion mass spectrometry (SIMS)

We used the CAMECA 1280-HR instrument housed in Potsdam to conduct U–Pb geochronology determinations on zircon. Due to technical problems with the instrument's chilled water supply, it was necessary to split the data collection into two sessions.

Our analytical method followed that of Ashwal et al. (2017). Briefly, our SIMS U–Pb analyses employed a 6 nA, $^{16}\text{O}_2^-$ primary ion beam operated in Köhler mode and with a total impact energy of 23 keV, resulting in a beam diameter of approximately 25 μm on the sample's surface. Oxygen flooding was used to enhance lead sensitivity, with the total pressure in the sample chamber maintained at $\sim 2 \times 10^{-3}$ Pa throughout both analytical sessions. Each analysis was preceded by a 6 nA, 70 s pre-sputtering of the target domain employing a 25 μm raster, which locally removed the gold coating, suppressed any surface contamination and helped establish equilibrium sputtering conditions. After completing the pre-sputtering, centring routines were applied to the

secondary beam that automatically scanned the sample high voltage, the field aperture in both the X and Y directions and, finally, corrected for any secondary magnetic field drift using the $^{90}\text{Zr}_2^{16}\text{O}$ mass station. Data were acquired using an ETP electron multiplier operating in mono-collection mode. A single analysis consisted of 12 cycles of the peak stepping sequence: $^{90}\text{Zr}_2^{16}\text{O}$ (1 s integration time per cycle), $^{92}\text{Zr}_2^{16}\text{O}$ (1 s), 200.5 (4 s), $^{94}\text{Zr}_2^{16}\text{O}$ (1 s), ^{204}Pb (6 s), ^{206}Pb (4 s), ^{207}Pb (6 s), ^{208}Pb (2 s), $^{177}\text{Hf}^{16}\text{O}_2$ (1 s), ^{232}Th (2 s), ^{238}U (2 s), $^{232}\text{Th}^{16}\text{O}$ (2 s), $^{238}\text{U}^{16}\text{O}$ (2 s), and $^{238}\text{U}^{16}\text{O}_2$ (2 s). Thus, including pre-sputtering, a single such analysis lasted approximately 12 min. Data were filtered for gross outliers at the three standard deviation level within each run. During both U–Pb analytical sessions, the entrance slits of the SIMS were set at 75- μm width, equivalent to a mass resolution of $M/\Delta M \approx 4200$ at 10% maximum peak height. The typical count rate for $^{90}\text{Zr}_2^{16}\text{O}$ under these conditions was $1\text{--}2 \times 10^4$ counts per second, to which a 46.2-ns dead time correction was applied to our ion counting system, as defined by a delay line in the electron multiplier's pre-amplifier circuit. The U–Pb age calibration for the machine was based on the zircon reference material 91500 ($^{206}\text{Pb}/^{238}\text{U}$ age: $1,062.4 \pm 0.4$ Ma; $^{207}\text{Pb}/^{206}\text{Pb}$ age: $1,065.4 \pm 0.3$; Wiedenbeck et al. 1995) with the Plešovice reference material ($^{206}\text{Pb}/^{238}\text{U}$ age: 337.13 ± 0.37 Ma; Sláma et al. 2008) used as a quality control material to evaluate the accuracy and stability of the U/Pb calibration measurements. Over the two sessions, a total of 90 measurements were made on the reference materials and a further 86 on the unknowns.

Data reduction employed the Excel-based program “NordAge” (M. Whitehouse, NORDSIM facility, Stockholm). The measurements done on the 91500 primary reference material were used to establish the inter-element fractionation using a Pb/UO vs. UO_2/UO calibration fitted with a power law function, from which individual best-fit curves were determined for both sessions. As an additional means of verifying the robustness of our calibration approach, $^{206}\text{Pb}/^{238}\text{U}$ ages of 1061.7 ± 2.0 Ma (1 SD, $N=41$) and 1062.3 ± 2.1 Ma (1 SD, $N=10$) were calculated for the 91500 reference material in sessions 1 and 2, respectively. The Plešovice quality control material gave mean $^{206}\text{Pb}/^{238}\text{U}$ ages of 341.4 ± 1.4 Ma (1 SD, $N=11$) and 340.6 ± 1.9 Ma (1 SD, $N=5$) for the two data collection sessions, respectively. Hence, as expected 91500 is within uncertainty of its assigned $^{206}\text{Pb}/^{238}\text{U}$ age of 1062.4 Ma, whereas our mean Plešovice results are slightly older than this material's published $^{206}\text{Pb}/^{238}\text{U}$ age of 337.13 Ma. We have checked in detail both our common Pb correction method as well as the UO_2/UO power law calibration scheme, but we have been unable to find any unusual features to these parts of our data reduction process. Thus, we are unable to explain the *circa* 4-Ma offset between the assigned age of our quality control material and the results of our measurements. We

have no reason to suppose the age results for the five samples investigated here also suffer from a *circa* 1% bias in their $^{206}\text{Pb}/^{238}\text{U}$ ages, but this possibility cannot be totally discounted.

The software package Isoplot (Ludwig 2012), was used to plot the U–Pb results using the decay constants recommended by the IUGS sub-commission on geochronology (Steiger and Jäger 1977). The isotope ratios and ages reported in Table 1 and Appendix 2 have an analytical uncertainty of 1 SD, whereas the uncertainty ellipses plotted in Fig. 4 are at the 2 SD level. During data evaluation, some analyses were found to suffer clearly from overcounts on the ^{204}Pb mass station. We therefore elected for most samples to employ a ^{208}Pb correction for correcting for the non-radiogenic component. The single exception to this strategy was for sample P (Pniewy), where the Th/U ratios appeared to have been disturbed, thereby preventing the use of a ^{208}Pb correction. In the case of sample P, we therefore did not apply any common Pb correction, and this approach appears justified based on the raw data which point to a nearly pure radiogenic Pb content in this particular case.

We also used the Potsdam CAMECA 1280-HR instrument to perform $\delta^{18}\text{O}$ determinations on zircon, largely following the method described in Nasdala et al. (2016). Briefly, the SIMS analyses employed a 2.5 nA, $^{133}\text{Cs}^+$ primary ion beam with a Gaussian intensity distribution with a total impact energy of 20 keV which was rastered over a 10

μm area with the dynamic transfer circuitry activated. Negative secondary ions were extracted using a -10 kV potential as applied to the sample holder, to which no offset voltage was applied, in conjunction with a 30 eV wide energy window, the position of which was mechanically centred at the beginning of the analytical session. Each analysis was preceded by a 2.5 nA, 60 s pre-sputtering of the target domain with a 20 μm raster. Total pressure in the source chamber varied between 1.4×10^{-6} and 3.2×10^{-6} Pa, throughout the first session, and 8.5×10^{-7} to 1.4×10^{-6} Pa during the second session. After completing the pre-sputtering, automatic centring routines were applied to the secondary beam in both the X and Y directions on the field and contrast apertures using the $^{16}\text{O}^-$ mass station. The instrument was operated in FC–FC multi-collection mode with the secondary magnetic field being fixed using the NMR sensor. The L2' ($^{16}\text{O}^-$) and the H2' ($^{18}\text{O}^-$) Faraday cups employed $10^{10}\ \Omega$ and $10^{11}\ \Omega$ resistors, respectively. The ion count rate on the $^{16}\text{O}^-$ peak was typically in the range of 3.0 to 3.5 billion ions per second. A single analysis consisted of 20 independent integrations, each lasting 4 s. Hence, an entire analysis, including pre-sputtering and the centring routines, lasted approximately 150 s. Data were filtered at the 2 SD level for the 20 integrations within the individual run, and the results were found to be consistent with a Gaussian distribution. Machine calibration was based on the 91500 zircon reference material (Wiedenbeck et al. 2004). The 91500 reference material was

Table 1 Compilation of zircon ages determined during this and previous studies (for details of this study, see also Fig. 4, Appendixes 2a and 2b)

Locality	Magmatic age (Ma) (published ^d)	Magmatic age (Ma) (this study ^d)	Inherited ages (Ma) (published ^d)	Inherited $^{206}\text{Pb}/^{238}\text{U}$ ages (Ma) (this study ^d) ^e
Daszewo ^a	293.0 ± 1.2 ($N = 21$)	297 ± 1.1 concordia age ($N = 8$) MSWD = 2.2	726; 1260; 2094; 2344; ($N = 4$)	Not found
Wysoka Kamieńska ^a	294.6 ± 1.2 concordant age ($N = 18$)	302 ± 1.5 concordia age ($N = 16$) MSWD = 1.7 ^c	Not found	356 ($N = 1$)
Pniewy ^a	298.5 ± 1.7 ($N = 5$)	Spread along the Concordia curve $^{206}\text{Pb}/^{238}\text{U}$ age between 318–323	599; 984; 1020; ($N = 3$)	II groups I: 381; 368 (core) 363 (rim); ($N = 2$) II: 473; 624; 668; 1544 ($N = 4$)
Chrzypsko (rhyolite)	–	$^{206}\text{Pb}/^{238}\text{U}$ age ca. 302 ($N = 4$) – MSWD = 4.8	–	552; 1935 (core) 1724 (rim) ($N = 2$)
Chrzypsko (granite) ^b	302 ± 2 mean age (MSWD = 1.17) ($N = 18$)	305 ± 0.8 concordia age ($N = 8$) MSWD = 1.6	910 ($N = 1$)	866 (core) 611 (rim) ($N = 1$)

N number of grains

^aPublished ages from Breitzkreuz et al. (2007)

^bPublished ages from Żelaźniewicz et al. (2016)

^cThe uncertainties going up with n in Wysoka Kamieńska is attributed to its being a heterogeneous population, MSWD ranges from 1.6 to 2.2, the probability of concordance for the samples is within the range of 5%

^dUncertainty in the age reported at the 1 SD level

^eAges have been rounded up and errors not included, for details see text or Appendix 2

measured a total of 29 times in the first session and further ten times during the second session. The overall repeatability of the determined IMF was ± 0.18 and $\pm 0.24\%$ (1 SD), respectively, for our two sessions. All together data for 39 RMs (Appendix 3) and 103 unknowns were collected over 4 days of SIMS data acquisition. Three of the days were continuous; the last day however was not, because it was necessary to re-polish one mount in order to have a fresh surface on the piece of 91500 embedded within it. Hence, we treated the data as two independent sessions. Data reduction used $+9.86 \pm 0.11\%$ as the value for the $\delta^{18}\text{O}_{\text{VSMOW}}$ value of 91500 (Wiedenbeck et al. 2004), for which we applied an $^{18}\text{O}/^{16}\text{O}$ ratio for VSMOW of 2.00520×10^{-3} (Baertschi 1976).

Laser ablation inductively coupled plasma mass spectrometry (LA-ICP-MS)

The acquisition of Lu–Hf data was performed at the University of Bristol (Bristol Isotope Group) using a Thermo Scientific™ Neptune multicollector ICP-MS coupled with a Photon-Machine Analyte G2 Excimer laser (193 nm wavelength). The beam diameter ranged from 40 to 50 μm depending on the grain size, and measurements were made using single circular spots, a laser frequency of 4 Hz, and an energy density of the laser beam of ca. 5.4 J/cm². A typical analysis lasted 90 s, including a 30-s background measurement and a 60-s ablation period. Since 50 μm spots produced smaller internal uncertainties than 40 μm spots, the former was preferred whenever the grain size allowed for its use. The spot sizes and placement within investigated zircons are presented in Appendix 1.

A procedure similar to those described in Kemp et al. (2009) and Pietranik et al. (2011) was applied to correct for the isobaric interference of ^{176}Yb on ^{176}Hf . The Yb mass bias was determined by measuring the $^{173}\text{Yb}/^{171}\text{Yb}$ ratio during each run and calculating the $^{176}\text{Yb}/^{177}\text{Hf}$ ratio using the natural $^{176}\text{Yb}/^{171}\text{Yb}$ ratio of 0.897145 (Segal et al. 2003). The ^{176}Lu abundance determination was based on measurements of ^{175}Lu that were then corrected using the natural abundance factor $^{175}\text{Lu}/^{176}\text{Lu} = 0.02655$ (Vervoort et al. 2004). According to a detailed study by Fisher et al. (2011), the Bristol Isotope Group's analytical method for Lu–Hf data acquisition and reduction provides accurate results for both natural and synthetic zircons with a large range of Yb/Hf ratios (typically $^{176}\text{Yb}/^{177}\text{Hf}$ from 0.001 to 0.3).

The $^{176}\text{Hf}/^{177}\text{Hf}$ values of three zircon reference materials measured during this study (Plešovice, Mud Tank and Temora2) are presented in Fig. 3. It appears that the Plešovice and Mud Tank $^{176}\text{Hf}/^{177}\text{Hf}$ values analysed in this study are in perfect agreement with the literature (for references see Fig. 3), whereas Temora2 gives slightly lower values. However, the lower values appear to be linked to

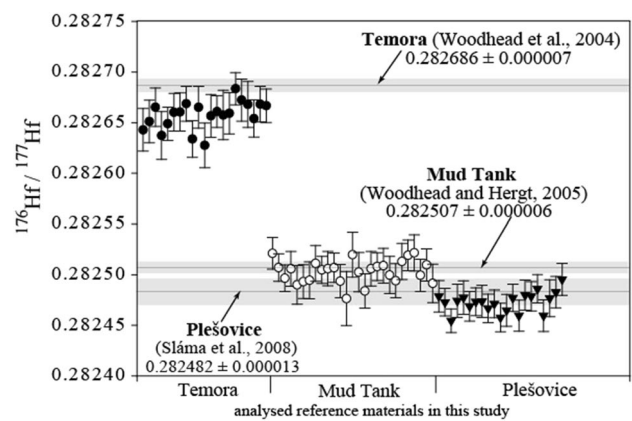


Fig. 3 LA-ICP-MS Hf isotope data from the Plešovice, Mud Tank and Temora II reference materials (uncertainty estimates on individual analyses are 2 SD)

analyses on newly sampled Temora II grains shipped from Australia within the last 2 years. Other Neptune users in Bristol have reported a similar problem, where they were getting consistently lower values for “new” Temora2 grains compared to older pieces (Bruand: personal communication 2015). Therefore, we interpret the slightly lower $^{176}\text{Hf}/^{177}\text{Hf}$ values for ‘new’ Temora2 as likely due to genuine heterogeneity. Chondritic uniform reservoir (CHUR) values of Bouvier et al. (2008) and ^{176}Lu decay value of Söderlund et al. (2004) were used to calculate ϵHf .

Results

Age and composition of zircons from the Polish Lowlands

The zircon grains from all four of our localities are characterized by irregular shapes, with rare oscillatory zonation (BSE images in Appendix 1).

Daszewo (rhyolite)

Fourteen zircon grains were dated from this sample, all of which were magmatic, with no inherited grains being detected. Eight zircons gave a mean concordia age of 297 ± 1.1 Ma (1 SD; Fig. 4a; Table 1). The six remaining grains were slightly discordant, but together, all 14 grains give a $^{206}\text{Pb}/^{238}\text{U}$ weighted average age of 297 ± 3 Ma. $\delta^{18}\text{O}_{\text{SMOW}}$ values measured on 12 of the grains (two of which were measured for both core and rim $\delta^{18}\text{O}$) ranged from 7.3 to 8.8‰, whereas ϵHf values determined for seven grains were between -8.5 and -9.8 . We found no correlation between $\delta^{18}\text{O}$ and ϵHf (Fig. 5). Th/U ratios

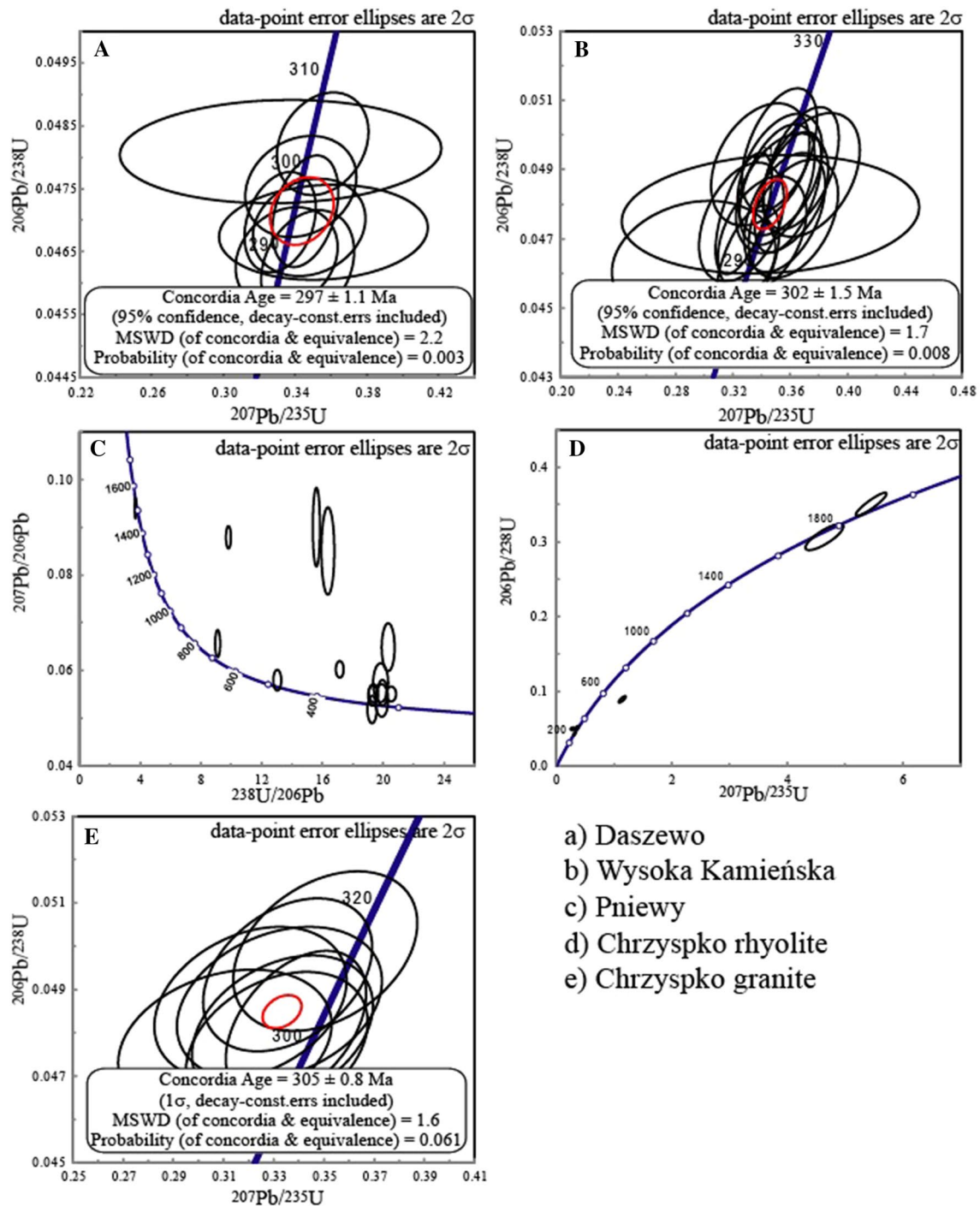


Fig. 4 U–Pb concordia plots of the Polish Lowlands zircons. For details see Appendix 2

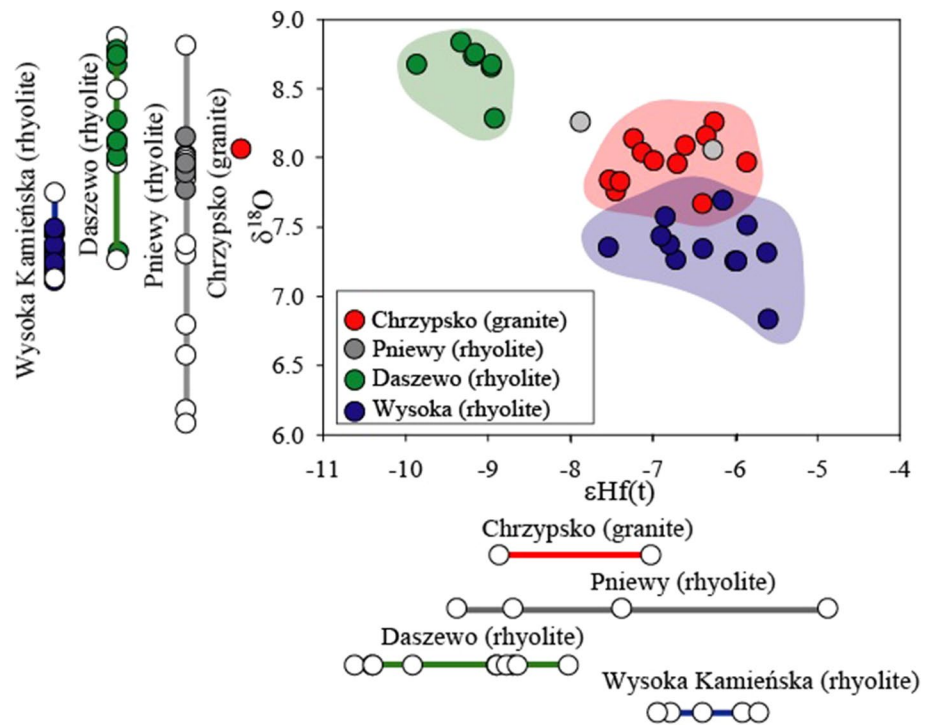
for the analysed grains are between 0.44 and 0.64 and the Hf concentrations varies between 8000 and 12,500 $\mu\text{g/g}$.

Wysoka Kamińska (rhyolite)

Twenty-nine zircon grains from this sample were dated, six of which having been evaluated on both the core and rim.

Of the 29 grains there was a single inherited grain dated at 355.5 ± 5.1 Ma. Not all the grains were concordant. The 16 grains that could be used to calculate a concordia age gave a mean age of 302 ± 1.5 Ma (Fig. 4b), whereas a weighted average $^{206}\text{Pb}/^{238}\text{U}$ age of 301 ± 5 Ma was calculated for the full suite of grains (Appendix 2b). $\delta^{18}\text{O}$ for 19 zircon grains (of those, nine had both core and rim analysed) giving

Fig. 5 Variations in $\delta^{18}\text{O}$ relative to ϵHf for zircons from the Polish Lowlands. Only grains < 315 Ma, and which have been analysed for both Hf and O isotopes are included in this plot. The ranges shown along the x and y axes represent the grains in which either $\delta^{18}\text{O}$ or ϵHf or the age were not analysed. Closed circles represent zircons where the age is known, whereas open circles are zircons without age determinations



values ranging from 6.2 to 7.7‰. ϵHf values for 12 magmatic grains lie between -5.6 and -7.7 . Thus in this case, the $\delta^{18}\text{O}$ values increase with a corresponding decrease in the ϵHf values (Fig. 5). The Th/U ratio varies between 0.31 and 0.57 and the Hf concentration varies from 8000 to 13,000 $\mu\text{g/g}$.

Pniewy 3 (rhyolite)

The 14 zircon grains dated in this sample can be divided into: (1) those located on the concordia curve between 318 and 323 Ma ($N=6$; Fig. 4c); (2) those which are inherited (six grains); (3) the remaining two analyses which were not considered in the age calculations as they were too discordant. The inherited grains are further subdivided into two groups: group I with younger ages of ~ 370 Ma: 381.3 ± 2.4 ; 367.6 ± 3.6 (core); 362.7 ± 2.4 (rim), and group II with the $^{206}\text{Pb}/^{238}\text{U}$ older ages of: 473 ± 3.7 , 624.3 ± 4.4 , 668 ± 4.5 and 1543.6 ± 9 Ma. The five most concordant grains in the 318–323 Ma population gave $\delta^{18}\text{O}$ ratios ranging from 7.51 to 8.26‰. ϵHf was measured on two of these ca. 320-Ma grains, and the results range from -6.3 to -7.9 . As only two grains from this locality have both $\delta^{18}\text{O}$ and ϵHf results, we cannot assess whether there is any correlation between these isotopic systems. The Hf concentration measured in magmatic rims on inherited varies from 10,500 to 12,500 $\mu\text{g/g}$.

Chrzypsko (rhyolite)

This sample yielded only a few grains, resulting in just four zircons being dated; however for three of which it was possible to date both the core and the rim (Fig. 4d). Two inherited grains are present; the first has a $^{206}\text{Pb}/^{238}\text{U}$ age of 552.2 ± 10.1 Ma, whereas the core of the second inherited grain gave a date of 1934.6 ± 30.6 Ma, with a younger rim age of 1724.2 ± 35.4 Ma. No concordia age could be calculated from the four dated grains as they did not form a tight enough statistical group; nevertheless, a $^{206}\text{Pb}/^{238}\text{U}$ weighted average age of ca. 302 Ma could be determined, but with so few measurements this age can only be considered as a rough indication (Appendix 2b). Due to the large uncertainty in the true age for Chrzypsko no further isotopic measurements were conducted on this sample.

Chrzypsko (granite)

Fourteen grains from this sample were dated, only one of which appears to be inherited (G_12; $^{206}\text{Pb}/^{238}\text{U}$ age of core 865.7 ± 11.8 Ma; age of rim 611 ± 8.7 Ma). One grain (G_1; Appendix 2) gave a younger $^{206}\text{Pb}/^{238}\text{U}$ age of 277.7 ± 4.8 Ma. Eight zircon grains give a mean age of 305 ± 0.8 Ma (Fig. 4e), with the data point ellipses plotting just to the left of the Concordia. This shift can be explained by a possible overestimate of the level of common Pb in the sample, which would result in a slight over correction.

A $^{206}\text{Pb}/^{238}\text{U}$ weighted average age of 303 ± 4 Ma was calculated for 12 grains (excluding the younger grain as well as the inherited grain; Appendix 2b). The $\delta^{18}\text{O}$ values for these magmatic grains (with two grains analysed for both core and rim) have values between 7.7 and 8.3‰. The ϵHf values determined for the same zircons give values between -6.3 and -7.9 . Thus, we detected no correlation between the ϵHf and $\delta^{18}\text{O}$ values for this sample (Fig. 5). The magmatic zircons have Th/U ratios between 0.42 and 0.69 and Hf concentrations between 7500 and 13,500 $\mu\text{g/g}$.

Discussion

Inherited and magmatic zircon ages: insight into potential magma sources of rhyolitic magmas

Late Paleozoic rhyolites from the Polish Lowlands can be divided into two groups based on the proportion of inherited and xenocrystic grains to magmatic zircon (autocrysts + antecrysts). We define inherited zircons as those surviving from the protolith melt source, whereas xenocrystic grains were those derived from external material during the evolution of magmatic system. Autocrysts and antecrysts refer to crystals that originate in the same magma system but antecrysts may represent slightly older episodes of the system formation and evolution, whereas autocrysts are related to the youngest magmatic episode (after Miller et al. 2007; Schmitt 2011). We do not attempt to distinguish autocrystic from antecrystic grains, because it requires a full dataset of whole rock and zircon trace element composition (Siégl et al. 2017), which was not obtained in this study. In this study the division between the northern and southern rhyolites is based on the relative proportion between pre-Permian/Upper Carboniferous and older zircons. Rhyolites from the northern part of the Polish Lowlands (Daszewo and Wysoka Kamińska) contain only a few older zircons, whereas rhyolites from the southern part (Pniewy and Chrzypsko) are dominated by such zircons (Table 1). Similar proportions between inherited and magmatic grains across the Polish Lowlands were also reported by Breitrkreuz et al. (2007; Table 1). This suggests differences exist between the sources for the respective rhyolites and that the pre-Permian basement in the northern and southern parts may differ. This is also consistent with the Hf and O isotope record (see “Discussion” below).

The zircon age distributions in southern and northern rhyolites shed light on the nature of the magma source. With regards to older than 300-Ma zircon ages, southern rhyolites (both the Pniewy and Chrzypsko) contain many zircons with ages 320–380 Ma in addition to individual zircons with ages ranging from ca. 500 Ma to 2.0 Ga. Interestingly, even though the ages are Variscan, the range in ages exceeds

that observed in igneous rocks of the Sudetes Mountains, which are between 300 and 350 Ma (e.g. Turniak et al. 2014; Oberc-Dziedzic et al. 2015; Kryza et al. 2012; Kusiak et al. 2014; Pietranik et al. 2013b; Białek and Werner 2004). This abundance of older zircon grains in the southern part of the Polish Lowlands with Variscan ages indicates that the source for these rhyolitic magmas was probably a sediment derived from the Variscan foreland (after 320 Ma). A Variscan-aged sedimentary source is also favoured by both geophysical evidence and by the analysis of drill cores showing monotonous series of turbidites deposited as a flysch during Tournasian (?) to Westphalian times (358–305 Ma, respectively) (Mazur et al. 2006). Consequently, our data suggest that the Variscan foreland could extend over the TESZ, in agreement with previous studies (Mazur et al. 2010, 2015). In particular, there is excellent agreement between the ages of inherited zircon in the Pniewy and Chrzypsko rhyolites and the zircon dated from the Carboniferous sandstones in the Września IG-1 well, which lies in close proximity to Pniewy and Chrzypsko (Mazur et al. 2010). Both Variscan (320–380 Ma) and 500–600 Ma ages are observed in zircon from turbidites and as inherited ages of rhyolitic zircon in this study. Altogether, this suggests that the Carboniferous foreland sediments were a primary source of rhyolitic magmas in the southern part of the studied area. However, scarce pre-Variscan zircon have ages typical for Avalonia or Baltica (ca. 620, 1350 Ma, two grains with 1490, 1800 Ma) and not Gondwana, which should not contain inherited ages between 1000 and 2000 Ma (e.g. Breitrkreuz et al. 2007; Pietranik et al. 2013a; Żelaźniewicz et al. 2016; Franke and Dulce 2017). Therefore, a mixture of sediments derived from several crustal blocks is favoured as the source of Pniewy and Chrzypsko rhyolites, with Variscan foreland sediments being the dominating source.

The source of the magmas that formed the northern rhyolites may be associated with the drilled lithologies present in the northern part of the Polish Lowlands. Consolidated pre-Permian sediments were sampled close to Daszewo locality. Several drill cores sampled Lower Paleozoic deposits of the Koszalin–Chojnice zone, including Ordovician fine-grained siliciclastic rocks (mostly hemipelagic massive or poorly laminated mudstones and claystones), which are associated with small amounts of carbonates, and Silurian deep-marine siliciclastic sediments (Podhalańska and Modliński 2006; Modliński and Podhalańska 2010; Mazur et al. 2017). These Paleozoic sediments are mostly fine-grained mudstones to siltstones; they contain rare sandstones with detrital zircon U/Pb SHRIMP ages indicative of their provenance from the East European Craton (clear dominance of zircon ages: 1756–2050, 1485–1510, and 974–1227 Ma over zircons from peri-Gondwanian terranes: 559–623 Ma and Caledonian U/Pb ages: 442–495 Ma); (Poprawa et al. 2006). Rhyolites from the Daszewo locality sampled during this study do

not contain any inherited zircon grains; however, inherited/xenocrystic zircon ages for Daszewo were reported by Breithkreuz et al. (2007) (see Table 1; ages: 726, 1260, 2094, 2344 Ma). These ages are in a very good agreement with the detrital ages from the sandstones. Neither this study, nor Breithkreuz et al. (2007) show zircon ages older than 350 Ma for rhyolites from Wysoka Kamieńska, suggesting that detrital zircon was scarce to absence in the source of these rhyolites. It is, therefore, probable that Paleozoic sediments contributed variable proportions to rhyolitic magmas and the scarcity of inherited grains in some rhyolites is due to a dominance of clay-rich sediments being generally impoverished in zircon compared to coarser grained sediments such as Carboniferous turbidites.

Therefore, based on the inherited to magmatic zircon proportions and zircon inherited ages, we suggest that the southern rhyolites were derived predominately from the Carboniferous turbidites with admixture of Baltica and/or Avalonia component, whereas northern rhyolites were derived from fine-grained sediments, poor in zircon, such as thick Ordovician–Sylurian sampled present in the Koszalin–Chojnice zone (Modliński and Podhalańska 2010).

Hafnium and oxygen isotopes: further insight into the sources of rhyolitic magmas

Magmatic zircons from rhyolites in the Polish Lowlands have distinctive Hf and O isotopic compositions (e.g., Daszewo, Wysoka Kamieńska as well as zircons from the Chrzypsko granite). Such a range in isotopic compositions may be surprising both considering that these rhyolites represent the same magmatic event and considering that their morphological and geochemical characteristics are roughly similar (Protas et al. 1995; Żelaźniewicz et al. 2016). This implies that chemically similar magmas were derived from isotopically variable sources and that the similar chemical composition of rhyolites likely reflects rather prolonged magma differentiation and it is not controlled by the source. The Hf and O isotope composition in the zircons not only confirms differences in the sources of the rhyolites from northern and southern parts of the Polish Lowlands, but also helps to distinguish additional sources in the northern part of the Polish Lowlands. Three distinct fields of Hf vs. O ratios (Fig. 5) suggest that different sources contributed to the magmatic evolution in these three areas.

Southern rhyolites

The composition of zircon from rhyolites of the southern part of the Polish Lowlands seems to overlap with that of zircon from the Chrzypsko granite; however, the southern rhyolites are represented only by two magmatic grains from the Pniewy ignimbrite (our sample of Chrzypsko rhyolite

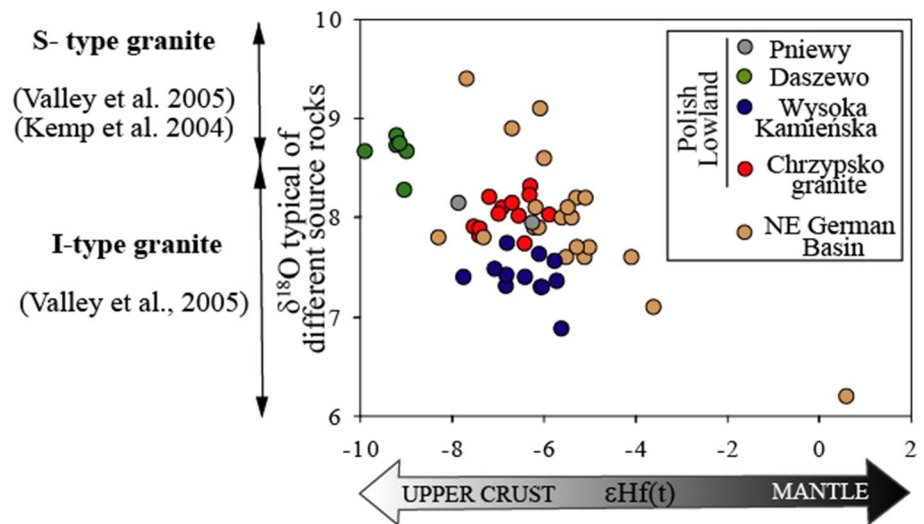
contained only inherited and xenocrystic zircons with no magmatic ones). Interestingly, the O isotopes for all the Variscan-aged grains (320–380 Ma) also overlap with the compositional field defined by the Chrzypsko granite (Fig. 5). Therefore, it seems that a single source dominated the production of the southern rhyolites and it was similar in composition to the Variscan magmas which are represented by the Chrzypsko granite and the Pniewy rhyolites. As Variscan-aged zircon grains are clearly found within the source of the Chrzypsko and Pniewy rhyolites, it is possible that the crustal component of this rhyolite magma was primarily derived from a fore-arc deposit, which formed due to the erosion of various Variscan igneous rocks in a hypothetical continental arc setting (Mazur et al. 2010). A derivation from a sedimentary source would explain the relatively high $\delta^{18}\text{O}$ values in the zircons from rhyolites in the southern part of Polish Lowlands as compared to the other Late Paleozoic rhyolites (e.g., Wysoka Kamieńska), but also compared to the Halle Volcanic Complex in eastern Germany (Ślodziński et al. 2016). Such high $\delta^{18}\text{O}$ values probably reflect a weathering of an igneous source before rhyolite magma formation, but because the sediment was deposited soon after erosion, it did not achieve typical sedimentary $\delta^{18}\text{O}$ values (Valley et al. 2005). Also the Hf isotope values for the granite and rhyolites in the Polish Lowlands are lower than those observed in most of the zircons derived from igneous rocks of the Bohemian Massif, which have ϵHf values from approximately -5 to 0 (e.g., Siebel and Chen 2009; Pietranik et al. 2011). This reflects the addition of low ϵHf materials to the southern rhyolites from the Polish Lowland, which suggests a larger contribution of sediments to the rhyolitic magmas compared to that of the mostly plutonic rocks in the Bohemian Massif.

Northern rhyolites

The possible sources for the northern rhyolites are more difficult to constrain. The lack of inherited grains may indicate scarce zircon in the source of magma, and such a source could be the Early Paleozoic, clay-rich sediments described by Podhalańska and Modliński (2006). However, it is clear that Daszewo and Wysoka Kamieńska represent two different compositional types of rhyolite derived from isotopically different sources. In detail:

- The high $\delta^{18}\text{O}$ and low ϵHf values for the Daszewo zircons suggest the involvement of (upper) crustal material of sedimentary origin as the source for these magmas (Fig. 6). The (meta-) sediments source is supported by the interpretation of electromagnetic data refraction within Pomeranian unit (Ernst et al. 2008) and may be correlated with Early Paleozoic siliciclastic rocks such as those described in the borehole in the Koszalin–Chojnice

Fig. 6 Comparison of $\delta^{18}\text{O}$ vs. ϵHf values for the Polish Lowlands samples and magmatic zircons from the NE German Basin (Pietranik et al. 2013a). The typical ranges in the isotopic ratios have been indicated



area (Podhalańska and Modliński 2006). Generally, high $\delta^{18}\text{O}$ values in combination with low ϵHf values suggest that the magma source might have been an old repeatedly recycled sediment, and as such, fits the characteristics of a typical passive margin deposit. Moreover, high $\delta^{18}\text{O}$ may record the influence of crustal brines interacting with the source rocks (Ernst et al. 2008), elevating their $\delta^{18}\text{O}$ as evaporates could have $\delta^{18}\text{O}$ as high as 20–30 delta units (Valley et al. 2005). The implication for such a source for the Daszewo rhyolites is consistent with the location of the drill hole over the attenuated margin of Baltica (Poprawa 2006; Żelaźniewicz et al. 2016; Mazur et al. 2017, Fig. 7b).

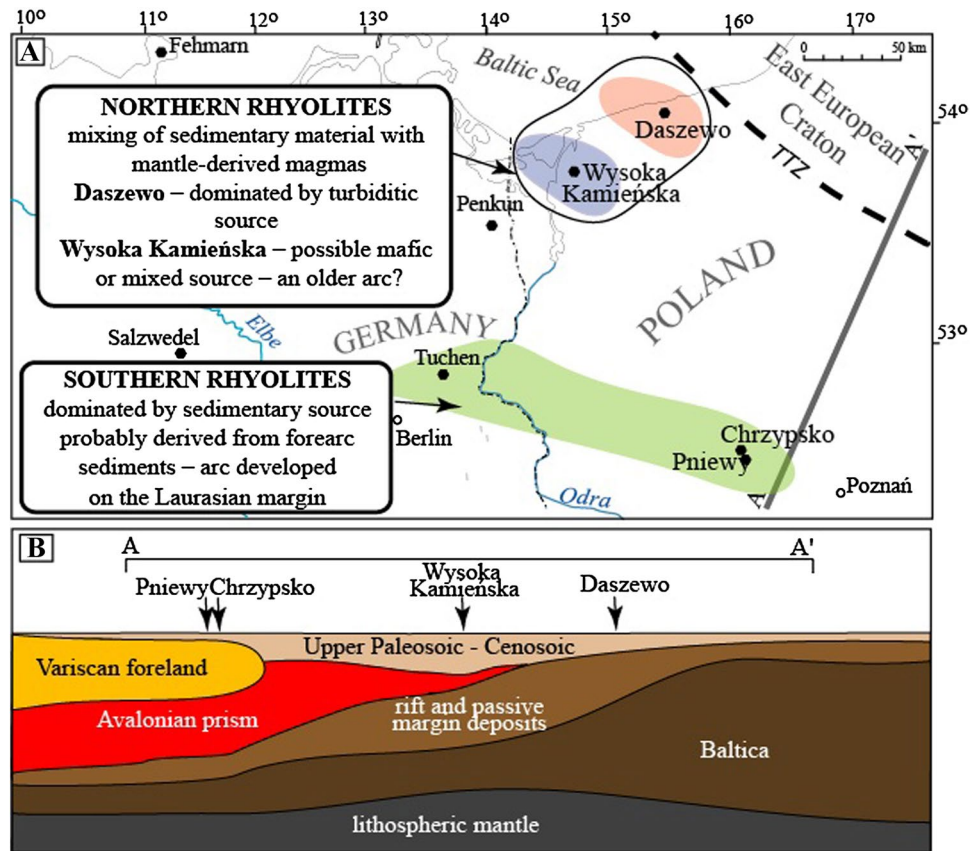
- Wysoka Kamińska is characterized by lower $\delta^{18}\text{O}$ and ϵHf values compared to Daszewo, which may correspond to more mafic components contributing to the source of these rhyolites (Fig. 6). In fact, both the Daszewo and Wysoka Kamińska zircon populations plot along the same linear trend in the $\delta^{18}\text{O}$ vs. ϵHf diagram (Fig. 5), suggesting a mixing of sedimentary material with mantle-derived magmas in both areas but with a larger input from the mantle-derived magmas in the Wysoka Kamińska rhyolite compared with the Daszewo rhyolite. Therefore, we propose that the isotopic difference between compositions of rhyolites from the two locations do not necessarily reflect the difference in the source area/tectonic setting, but rather varying admixtures between volcano-sedimentary successions in the source. However, the two successions may, in fact, reflect the presence of two distinct crustal blocks in the close proximity that contributed material to pre-Permian sediments i.e. the Baltica crustal block (these sediments dominate in Daszewo) and an Avalonian accretionary prism (these sediments dominate in Wysoka Kamińska).

It is interesting to note that each of the sampling localities plots in its own, rather limited, compositional field. As reported for large eruptable rhyolitic systems such as the Yellowstone Caldera (e.g. Stelten et al. 2015) or the German part of the Central European Basin Large Igneous Province (Pietranik et al. 2013a), the generation of such magmas involves at least two stages of melt evolution, first the extraction from a long-lived, isotopically heterogeneous crystal mush, and second the emplacement of a pre-eruptive, isotopically homogenized magma chamber. In such evolution scenarios chemical and isotope diversity is expected in zircon grains. The lack of such diversity, as is the case for the Polish Lowland zircons investigated here, may suggest the dominance of a single source in the formation of the rhyolites. Therefore, we stress the importance of the differences in the crustal material available for melting between the Daszewo and Wysoka Kamińska rhyolites as well as between the northern and southern parts of the Polish Lowlands.

Chrzypsko granite and rhyolite: are they related?

A large silicic magmatic system may persist within the crust as a long-lived mush with several episodes of rapid remobilization, which finally can crystallize into a granitic body or, alternatively, can feed a large eruption (e.g. Burgisser and Bergantz 2011). It is also possible that such a crystalline granitic body could be reheated from below, generating “new” portions of rhyolitic magma. The origin of voluminous high-silica ignimbrites by extraction from a shallow, batholithic sized granitic magma mush is one of the possible scenarios by which such volcanic systems are generated (see Lipman and Bachmann 2015). However, it seems not to be the case for rhyolitic and granitic samples investigated here. Despite the overall similarities in the Hf and O isotope composition

Fig. 7 **a** Map showing the spatial distribution of the rhyolites in the NE German Basin, which were previously analysed by Breitreuz et al. (2007) and Pietranik et al. (2013a) in addition to the rhyolites from the Polish Lowlands which were analysed during this study. The shaded area indicates the location of the northern and southern rhyolites as discussed in the text, TTZ Teisseyre–Tornquist Zone; **b** schematic cross section (not to scale) showing the structure of the Trans-European Suture Zone along line A–A' (model from Żelaźniewicz et al. 2016 modified after; Mazur et al. 2016; Smit et al. 2016). The approximate locations of the analysed samples have been indicated



between the Chrzypsko granite and the rhyolites from Chrzypsko and Pniewy in the south, the granite and volcanic rocks cannot be directly related. This is in part because the rhyolites contain abundant inherited and very scarce magmatic zircon grains, while in contrast the Chrzypsko granite contains few inherited but quite abundant magmatic zircons (Table 1). The only differentiation process which could enrich an evolving granitic pluton with inherited zircons is by the assimilation of the surrounding sedimentary or metasedimentary rocks. Such assimilation may happen when rhyolitic magma ascends through thick sedimentary sequence, however the process would have been possible for Chrzypsko granite/rhyolite only if the sediment did not contaminate magma itself. Sediments with distinct composition would likely change the isotopic composition of the evolving magma, which then should be recorded in magmatic zircon chemistry; such a process was not observed for the Chrzypsko locality. However, it is possible that the magma composition changed due to assimilation, but we did not sample a new magma composition, because no real rhyolitic magmatic zircon was present. Zircons with young ages could represent antecrystic component derived from granite and, therefore, have the same Hf and O isotope composition as the granitic zircon. Alternatively, it may be that the Pniewy and Chrzypsko rhyolites were not derived by the remelting and/or re-mobilization of the Chrzypsko granite,

but rather that both the granite and rhyolites originate from a common source rich in inherited zircons. The reason for the granite to then contain fewer inherited zircons is a matter of its thermal evolution in time, if the temperature in granite decreased slowly there would be a higher likelihood for the dissolution/melting of the inherited component. In contrast, if the rhyolitic magmas cooled quickly, they may have been more likely to preserve the inherited grains.

Comparing late paleozoic high silica magmas in the Polish Lowlands with those of the North East German Basin

As has already been established in previous sections, the rhyolites in the south contain a large number of inherited zircons, covering a wide range in ages. This is similar to the Tuchen rhyolite, which is located in the southern part of the North East German Basin (NEGB) (Fig. 7, Breitreuz et al. 2007). This suggests that the same sedimentary source which was melted to produce the Pniewy and Chrzypsko rhyolites may have extended further to the east, for at least another 100 km. Furthermore, the Hf and O isotopic compositional fields of the southern rhyolites and the rhyolites from Penkun and Salzswedel in the NEGB (Fig. 6, Pietranik et al. 2013a) partially overlap,

suggesting that similar processes could have acted in the evolution over this broad area. Conversely, because there is a small inherited component in the rhyolites found in the northern part of the Polish Lowlands, and their Hf and O isotopic compositions do not overlap with any of the zircons from the NEGB rhyolites, this implies that the rhyolites in the north formed under different conditions to those in the both south and within the NEGB—this might be due to a differences between the sediments that melted to form these rhyolites. One feature common to both the rhyolites in the Polish Lowlands and the NEGB are the magmatic zircons with $\delta^{18}\text{O}$ values consistently $> 6\text{‰}$. Such relatively high $\delta^{18}\text{O}$ values are also present in other large rhyolitic eruptions worldwide (e.g., Neogene Central Andean Ignimbrite Province; Folkes et al. 2013). However, many rhyolite localities preserve zircon with $\delta^{18}\text{O}$ of less than 5‰ , which has been interpreted as reflecting extensive remelting/recycling of hydrothermally altered intracaldera rhyolites (e.g., Snake River Plain in Idaho; Bindeman et al. 2008; Watts et al. 2011; Drew et al. 2013). The apparent absence of any hydrothermal alteration in the source of Andean rhyolites may have been related to climatic and geographical factors such as high elevation prior and during the eruption and lack of meteoric water input into lithosphere due to an arid climate. However, the Permian basin developed in an extensional setting and topographically elevated forms, even if they had been present, would not be expected to influence the climate to such a degree as to cause aridity of the region (Geißler et al. 2008). Therefore, we suggest that the lack of low $\delta^{18}\text{O}$ zircon in the case of both Polish Lowland and NE German Basin could be related to either the nature of the specific sources in conjunction with a large contribution of sedimentary material or to an arid climate specific for Lower Permian period (Gibbs et al. 2002; Roscher and Schneider 2006).

Conclusions

Late Paleozoic rhyolites from the Polish Lowlands offer insight into the composition and structure of the crust which makes up the Trans-European Suture Zone in Poland. Hf and O isotopic compositions of zircon, as well as the distribution of zircon ages show that the rhyolitic magmas were derived from three different sources: (1) older (Ordovician–Silurian) sediments in the case of Daszewo; these sediments were probably deposited on the passive margin of Baltica predominately as mudstone–siltstone sequences (cf. Modliński and Podhalańska 2010); (2) a mixed mantle or mafic crust-sediment source for the Wysoka Kamieńska rhyolites, perhaps mixing between magmas derived from the mudstone–siltstone

source similar to that implied for Daszewo and mafic arc rocks (an Avalonian accretionary prism); and (3) a younger, Variscan-aged coarser sediments for the Chrzypsko and Pniewy rhyolites, deposited on the Variscan foreland (Fig. 7), which could be related to Carboniferous greywackes (cf. Mazur et al. 2010). The rhyolites from the Polish Lowlands correlate with occurrences of similar rocks within the NE German Basin. Thus, during the Late Paleozoic, there was large scale magmatism in central Europe, and its composition was controlled by regional scale differences in the basement lithologies.

Acknowledgements We would like to thank Professor Teresa Oberc–Dziedzic for providing the Chrzypsko samples and Geonafra in Piła for providing the other samples. F. Couffignal was responsible for our SIMS data acquisition; U. Dittmann helped in producing the SIMS mounts; D. Rhede and F. Wilke helped with microprobe analyses. ES acknowledges financial support from the Polish National Science Centre Grant No. UMO-2013/09/N/ST10/00655.

Open Access This article is distributed under the terms of the Creative Commons Attribution 4.0 International License (<http://creativecommons.org/licenses/by/4.0/>), which permits unrestricted use, distribution, and reproduction in any medium, provided you give appropriate credit to the original author(s) and the source, provide a link to the Creative Commons license, and indicate if changes were made.

References

- Ashwal LD, Wiedenbeck M, Torsvik TH (2017) Archaean zircons in Miocene oceanic hotspot rocks establish ancient continental crust beneath Mauritius. *Nat Commun* 8:14086. <https://doi.org/10.1038/ncomms14086>
- Awdankiewicz M, Kryza R, Szczepara N (2013) Timing of post-collisional volcanism in the eastern part of the Variscan Belt: constraints from SHRIMP zircon dating of Permian rhyolites in the North-Sudetic Basin (SW Poland). *Geol Mag* 151:611–628. <https://doi.org/10.1017/s0016756813000678>
- Baertschi P (1976) Absolute ^{18}O content of standard mean ocean water. *Earth Planet Sci Letters* 31:341–344. [https://doi.org/10.1016/0012-821x\(76\)90115-1](https://doi.org/10.1016/0012-821x(76)90115-1)
- Benek R, Kramer W, McCann T, Scheck M, Negendank JF, Korich D, Huebcher H-D, Bayer U (1996) Permo-Carboniferous magmatism of the Northeast German Basin. *Tectonophysics* 266:379–404. [https://doi.org/10.1016/S0040-1951\(96\)00199-0](https://doi.org/10.1016/S0040-1951(96)00199-0)
- Białek D, Werner T (2004) Geochemistry and geochronology of the Javornik granodiorite and its geodynamic significance in the Eastern Variscan belt. *Geolines* 17:22–23
- Bindeman IN, Fu B, Kita NT, Valley JW (2008) Origin and evolution of silicic magmatism at Yellowstone based on Ion Microprobe analysis of isotopically zoned zircons. *J Petrol* 49:163–193. <https://doi.org/10.1093/petrology/egm075>
- Bouvier A, Vervoort JD, Patchett PJ (2008) The Lu–Hf and Sm–Nd isotopic composition of CHUR: constraints from unequilibrated chondrites and implications for the bulk composition of terrestrial planets. *Earth Planet Sci Lett* 273:48–57. <https://doi.org/10.1016/j.epsl.2008.06.010>
- Breitkreuz C, Kennedy A (1999) Magmatic flare-up at the Carboniferous/Permian boundary in the NE German Basin revealed by

- SHRIMP zircon ages. *Tectonophysics* 302:307–326. [https://doi.org/10.1016/S0040-1951\(98\)00293-5](https://doi.org/10.1016/S0040-1951(98)00293-5)
- Breitkreuz C, Kennedy A, Geißler M, Ehling B-C, Kopp J, Muszyński A, Protas A, Stouge S (2007) Far Eastern Avalonia: its chronostratigraphic structure revealed by SHRIMP zircon ages from Upper Carboniferous to Lower Permian volcanic rocks (drill cores from Germany, Poland, and Denmark). *Geol Soc Am Spec Pap* 432:173–190
- Burgisser A, Bergantz GW (2011) A rapid mechanism to remobilize and homogenize highly crystalline magma bodies. *Nature* 471:212–215. <https://doi.org/10.1038/nature09799>
- Dadlez R (2006) The Polish Basin—relationship between the crystalline, consolidated and sedimentary crust. *Geol Q* 50:43–58
- Dadlez R, Grad M, Guterch A (2005) Crustal structure below the Polish Basin: is it composed of proximal terranes derived from Baltica? *Tectonophysics* 411:111–128. <https://doi.org/10.1016/j.tecto.2005.09.004>
- Drew DL, Bindeman IN, Watts KE, Schmitt AK, Fu B, McCurry M (2013) Crustal-scale recycling in caldera complexes and rift zones along the Yellowstone hotspot track: O and Hf isotopic evidence in diverse zircons from voluminous rhyolites of the Picabo volcanic field, Idaho. *Earth Planet Sci Lett* 381:63–77. <https://doi.org/10.1016/j.epsl.2013.08.007>
- Ernst T, Brasse H, Cerv V, Hoffmann N, Jankowski J, Jóźwiak W, Kreutzmann A, Neska A, Palshin N, Pedersen LB, Smirnov M, Sokolova E, Varentsov IM (2008) Electromagnetic images of the deep structure of the Trans-European Suture Zone beneath Polish Pomerania. *Geophys Res Lett* 35:L15307. <https://doi.org/10.1029/2008gl034610>
- Fisher CM, Hanchar JM, Samson SD, Dhuime B, Blichert-Toft J, Vervoort JD, Lam R (2011) Synthetic zircon doped with hafnium and rare earth elements: a reference material for in situ hafnium isotope analysis. *Chem Geol* 286:32–47. <https://doi.org/10.1016/j.chemgeo.2011.04.013>
- Folkes CB, Silva SL de, Bindeman IN, Cas RAF (2013) Tectonic and climate history influence the geochemistry of large-volume silicic magmas: new $\delta^{18}\text{O}$ data from the Central Andes with comparison to N America and Kamchatka. *J Volcanol Geotherm Res* 262:90–103. <https://doi.org/10.1016/j.jvolgeores.2013.05.014>
- Franke W, Dulce J-C (2017) Back to sender: tectonic accretion and recycling of Baltica-derived Devonian clastic sediments in the Rheno-Hercynian Variscides. *Int J Earth Sci* 106:377–386. <https://doi.org/10.1007/s00531-016-1408-y>
- Geißler M, Breitkreuz C, Kiersnowski H (2008) Late Paleozoic volcanism in the central part of the Southern Permian Basin (NE Germany, W Poland): facies distribution and volcano-topographic hiatus. *Int J Earth Sci* 97:973–989. <https://doi.org/10.1007/s00531-007-0288-6>
- Gibbs MT, Rees PM, Kutzbach JE, Ziegler AM, Behling PJ, Rowley DB (2002) Simulations of Permian climate and comparisons with climate-sensitive sediments. *J Geol* 110:33–55. <https://doi.org/10.1086/324204>
- Goolaerts A, Mattioli N, Jong J de, Weis D, Scoates JS (2004) Hf and Lu isotopic reference values for the zircon standard 91500 by MC-ICP-MS. *Chem Geol* 206:1–9. <https://doi.org/10.1016/j.chemgeo.2004.01.008>
- Grad M, Polkowski M (2016) Seismic basement in Poland. *Int J Earth Sci* 105:1199–1214. <https://doi.org/10.1007/s00531-015-1233-8>
- Grad M, Guterch A, Mazur S (2003) Seismic refraction evidence for crustal structure in the central part of the Trans-European Suture Zone in Poland. *Geol Soc Lond Spec Publ* 201:295–309. <https://doi.org/10.1144/gsl.sp.2002.201.01.14>
- Grad M, Guterch A, Keller GR, Janik T, Hegedűs E, Vozár J, Ślaczka A, Tiira T, Yliniemi J (2006) Lithospheric structure beneath trans-Carpathian transect from Precambrian platform to Pannonian basin: CELEBRATION 2000 seismic profile CEL05. *J Geophys Res Solid Earth*. <https://doi.org/10.1029/2005jb003647>
- Grad M, Guterch A, Polkowska-Purys A (2012) Crustal structure of the Trans-European Suture Zone in Central Poland—reinterpretation of the LT-2, LT-4 and LT-5 deep seismic sounding profiles. *Geol Q* 49:243–252
- Guterch A, Grad M (2010) Lithospheric structure of the TESZ in Poland based on modern seismic experiments. *Geol Q* 50:23–32
- Haydukiewicz J, Muszer J, Kłapiński J (1999) Palaeontological documentation of the sub-Permian sediments in the vicinity of Zbąszyń (Fore-Sudetic Monocline). *Selected Problems of Stratigraphy, Tectonics and Ore Mineralization in Lower Silesia*; pp 7–17
- Hoffmann U, Breitkreuz C, Breiter K, Sergeev S, Stanek K, Tichomirowa M (2012) Carboniferous–Permian volcanic evolution in Central Europe—U/Pb ages of volcanic rocks in Saxony (Germany) and northern Bohemia (Czech Republic). *Int J Earth Sci* 102:73–99. <https://doi.org/10.1007/s00531-012-0791-2>
- Jackowicz E (1994) Permskie skały wulkaniczne północnej części monokliny przedsudeckiej. *Prace Państwowego Instytutu Geologicznego* 145:1–47 (**In Polish, English abstract**)
- Jóźwiak W (2013) Electromagnetic study of lithospheric structure in the marginal zone of East European Craton in NW Poland. *Acta Geophys* 61:1101–1129. <https://doi.org/10.2478/s1160-0-013-0127-z>
- Kemp AIS, Foster GL, Scherstén A, Whitehouse MJ, Darling J, Storey C (2009) Concurrent Pb–Hf isotope analysis of zircon by laser ablation multi-collector ICP-MS, with implications for the crustal evolution of Greenland and the Himalayas. *Chem Geol* 261:244–260. <https://doi.org/10.1016/j.chemgeo.2008.06.019>
- Kiersnowski H, Paul J, Peryt TM, Smith DB (1995) Facies, paleogeography, and sedimentary history of the Southern Permian Basin in Europe. In: *The Permian of Northern Pangea*. Springer, Berlin, pp 119–136
- Kryza R, Awdankiewicz M (2012) Ambiguous geological position of Carboniferous rhyodacites in the Intra-Sudetic Basin (SW Poland) clarified by SHRIMP zircon ages. *Geol Q* 56:55–66
- Kryza R, Crowley QG, Larionov A, Pin Ch, Oberc-Dziedzic T, Mochnacka K (2012) Chemical abrasion applied to SHRIMP zircon geochronology: an example from the Variscan Karkonosze Granite (Sudetes, SW Poland). *Gondwana Res* 21:757–767. <https://doi.org/10.1016/j.gr.2011.07.007>
- Kusiak MA, Williams IS, Dunkley DJ, Konečný P, Słaby E, Martin H (2014) Monazite to the rescue: U–Th–Pb dating of the intrusive history of the composite Karkonosze pluton, Bohemian Massif. *Chem Geol* 364:76–92. <https://doi.org/10.1016/j.chemgeo.2013.11.016>
- Lipman PW, Bachmann O (2015) Ignimbrites to batholiths: integrating perspectives from geological, geophysical, and geochronological data. *Geosphere* 11:705–743. <https://doi.org/10.1130/ges01091.1>
- Littke R, Bayer U, Gajewski D (2005) Dynamics of sedimentary basins: the example of the Central European Basin system. *Int J Earth Sci* 94:779–781. <https://doi.org/10.1007/s00531-005-0036-8>
- Ludwig KR (2012) *Isoplot/Ex*, v. 3.75, Berkeley Geochronol, 5. Center, Spec Publ
- Maliszewska A, Kiersnowski H, Jackowicz E (2003) Wulkanoklastyczne osady czerwonego spagowca dolnego na obszarze Wielkopolski. *Prace Państwowego Instytutu Geologicznego* 179 (**In Polish, English, abstract**)
- Matyja H (2006) Stratygrafia i rozwój facjalny osadów dewonu i karbonu w basenie pomorskim i w zachodniej części basenu bałtyckiego a paleozoiczna paleogeografia północnej części TESZ. *Prace Państwowego Instytutu Geologicznego* 186:79–122 (**In Polish, English abstract**)
- Mazur S, Dunlap WJ, Turniak K, Oberc-Dziedzic T (2006) Age constraints for the thermal evolution and erosional history of the

- central European Variscan belt: new data from the sediments and basement of the Carboniferous foreland basin in western Poland. *J Geol Soc* 163:1011–1024. <https://doi.org/10.1144/0016-76492004-170>
- Mazur S, Aleksandrowski P, Turniak K, Krzemiński L, Mastalerz K, Górecka-Nowak A, Kurowski L, Krzywiec P, Żelaźniewicz A, Fanning MC (2010) Uplift and late orogenic deformation of the Central European Variscan belt as revealed by sediment provenance and structural record in the Carboniferous foreland basin of western Poland. *Int J Earth Sci* 99:47–64. <https://doi.org/10.1007/s00531-008-0367-3>
- Mazur S, Mikołajczak M, Krzywiec P, Malinowski M, Buffenmyer V, Lewandowski M (2015) Is the Teisseyre–Tornquist Zone an ancient plate boundary of Baltica? *Tectonics* 34:2465–2477. <https://doi.org/10.1002/2015TC003934>
- Mazur S, Mikołajczak M, Krzywiec P, Malinowski M, Lewandowski M, Buffenmyer V (2016) Pomeranian Caledonides, NW Poland—A collisional suture or thin-skinned fold-and-thrust belt? *Tectonophysics* 692:29–43. <https://doi.org/10.1016/j.tecto.2016.06.017>
- Mazur S, Porębski SJ, Kędzior A, Paszkowski M, Podhalańska T, Poprawa P (2017) Refined timing and kinematics for Baltica–Avalonia convergence based on the sedimentary record of a foreland basin. *Terra Nova*. <https://doi.org/10.1111/ter.12302>
- Miller JS, Matzel JEP, Miller CF, Burgess SD, Miller RB (2007) Zircon growth and recycling during the assembly of large, composite arc plutons. *J Volcanol Geotherm Res* 167:282–299. <https://doi.org/10.1016/j.jvolgeores.2007.04.019>
- Modliński Z, Podhalańska T (2010) Outline of the lithology and depositional features of the lower Paleozoic strata in the Polish part of the Baltic region. *Geol Q* 54:109–121
- Nasdala L, Corfu F, Valley JW, Spicuzza MJ, Wu F-Y, Li Q-L, Yang Y-H, Fisher C, Münker C, Kennedy AK, Reiners PW, Kronz A, Wiedenbeck M, Wirth R, Chanmuang C, Zeug M, Váczi T, Norberg N, Häger T, Kröner A, Hofmeister W (2016) Zircon M127—a homogeneous reference material for SIMS U–Pb geochronology combined with hafnium, oxygen and, potentially, lithium isotope analysis. *Geostand Geoanal Res* 40:457–475. <https://doi.org/10.1111/ggr.12123>
- Nawrocki J, Poprawa P (2006) Development of trans-European Suture Zone in Poland: from Ediacaran rifting to early Palaeozoic accretion. *Geol Q* 50:59–76
- Oberc-Dziedzic T, Kryza R, Pin C (2015) Variscan granitoids related to shear zones and faults: examples from the Central Sudetes (Bohemian Massif) and the Middle Odra Fault Zone. *Int J Earth Sci* 104:1139–1166. <https://doi.org/10.1007/s00531-015-1153-7>
- Paulick H, Breitzkreuz C (2005) The Late Paleozoic felsic lava-dominated large igneous province in northeast Germany: volcanic facies analysis based on drill cores. *Int J Earth Sci* 94:834–850. <https://doi.org/10.1007/s00531-005-0017-y>
- Pharaoh TC (1999) Palaeozoic terranes and their lithospheric boundaries within the Trans-European Suture Zone (TESZ): a review. *Tectonophysics* 314:17–41. [https://doi.org/10.1016/S0040-1951\(99\)00235-8](https://doi.org/10.1016/S0040-1951(99)00235-8)
- Pietranik A, Storey C, Dhuime B, Tyska R, Whitehouse M (2011) Decoding whole rock, plagioclase, zircon and apatite isotopic and geochemical signatures from variably contaminated dioritic magmas. *Lithos* 127:455–467. <https://doi.org/10.1016/j.litho.2011.10.002>
- Pietranik A, Słodczyk E, Hawkesworth CJ, Breitzkreuz C, Storey CD, Whitehouse M, Milke R (2013a) Heterogeneous zircon cargo in voluminous Late Paleozoic rhyolites: Hf, O isotope and Zr/Hf records of plutonic to volcanic magma evolution. *J Petrol* 54:1483–1501. <https://doi.org/10.1093/petrology/egt019>
- Pietranik A, Storey C, Kierczak J (2013b) The Niemcza diorites and monzodiorites (Sudetes, SW Poland): a record of changing geotectonic setting at ca. 340 Ma. *Geol Q* 57:325–334. <https://doi.org/10.7306/gq.1084>
- Podhalańska T, Modliński Z (2006) Stratigraphy and facies characteristics of the Ordovician and Silurian deposits of the Koszalin–Chojnice zone; similarities and differences to the western margin of the East European Craton and Rügen area. *Prace Państwowego Instytutu Geologicznego* 186:39–78 (**In Polish, English abstract**)
- Poprawa P (2006) Development of the Caledonian collision zone along the western margin of Baltica and its relation to the foreland basin. *Prace Państwowego Instytutu Geologicznego* 186:189–214 (**In Polish, English abstract**)
- Poprawa P, Paszkowski M, Fanning MC, Pécskay Z, Nawrocki J, Sikorska M (2006) Geochronological characteristics of source areas for the Lower Paleozoic sediments from the NW East European Craton and Koszalin–Chojnice zone; dating of detrital mica (K/Ar) and zircon (U/Pb SHRIMP). *Prace Państwowego Instytutu Geologicznego* 186:149–164 (**In Polish, English abstract**)
- Pożaryski W, Grocholski A, Tomczyk H, Karnkowski P, Moryc W (1992) Mapa tektoniczna Polski w epoce waryscyjskiej. *Przegląd geologiczny* 40:643 (Polish)
- Protas A, Biernacki J, Muszyński A, Wojewoda J (1995) Pozycja geologiczna i petrologia kompleksu wulkanicznego permu podłoża Pomorza Zachodniego (na podstawie otworów wiertniczych). Program badawczy komitetu badań naukowych No 6. P201 043 05 (**In Polish**)
- Roscher M, Schneider JW (2006) Permo-Carboniferous climate: early Pennsylvanian to Late Permian climate development of central Europe in a regional and global context. *Geol Soc Lond Spec Publ* 265:95–136. <https://doi.org/10.1144/gsl.sp.2006.265.01.05>
- Schmitt AK (2011) Uranium series accessory crystal dating of magmatic processes. *Annu Rev Earth Planet Sci* 39:321–349. <https://doi.org/10.1146/annurev-earth-040610-133330>
- Schoene B, Latkoczy C, Schaltegger U, Günther D (2010) A new method integrating high-precision U–Pb geochronology with zircon trace element analysis (U–Pb TIMS-TEA). *Geochim Cosmochim Acta* 74:7144–7159. <https://doi.org/10.1016/j.gca.2010.09.016>
- Schweitzer J (1995) Blockage of regional seismic waves by the Teisseyre–Tornquist zone. *Geophys J Int* 123:260–276. <https://doi.org/10.1111/j.1365-246x.1995.tb06674.x>
- Segal I, Halicz L, Platzner IT (2003) Accurate isotope ratio measurements of ytterbium by multiple collection inductively coupled plasma mass spectrometry applying erbium and hafnium in an improved double external normalization procedure. *J Anal Atom Spectrom* 18:1217. <https://doi.org/10.1039/b307016f>
- Siebel W, Chen F (2009) Zircon Hf isotope perspective on the origin of granitic rocks from eastern Bavaria, SW Bohemian Massif. *Int J Earth Sci* 99:993–1005. <https://doi.org/10.1007/s00531-009-0442-4>
- Siégl C, Bryan SE, Allen CM, Gust DA (2017) Use and abuse of zircon-based thermometers: a critical review and a recommended approach to identify antecrystic zircons. *Earth Sci Rev* 176:87–116. <https://doi.org/10.1016/j.earscirev.2017.08.011>
- Sláma J, Košler J, Condon DJ, Crowley JL, Gerdes A, Hanchar JM, Horstwood MSA, Morris GA, Nasdala L, Norberg N, Schaltegger U, Schoene B, Tubrett MN, Whitehouse M (2008) Plešovice zircon—a new natural reference material for U–Pb and Hf isotopic microanalysis. *Chem Geol* 249:1–35. <https://doi.org/10.1016/j.chemgeo.2007.11.005>
- Słodczyk E, Pietranik A, Breitzkreuz C, Fanning CM, Anczkiewicz R, Ehling B-C (2016) Rhyolite magma evolution recorded in isotope and trace element composition of zircon from Halle Volcanic Complex. *Lithos* 248–251:402–417. <https://doi.org/10.1016/j.litho.2016.01.029>

- Smit J, Wees J-D van, Cloetingh S (2016) The Thor suture zone: from subduction to intraplate basin setting. *Geology* 44:707–710. <https://doi.org/10.1130/g37958.1>
- Söderlund U, Patchett PJ, Vervoort JD, Isachsen CE (2004) The ^{176}Lu decay constant determined by Lu–Hf and U–Pb isotope systematics of Precambrian mafic intrusions. *Earth Planet Sci Lett* 219:311–324. [https://doi.org/10.1016/s0012-821x\(04\)00012-3](https://doi.org/10.1016/s0012-821x(04)00012-3)
- Steiger RH, Jäger E (1977) Subcommission on geochronology: convention on the use of decay constants in geo- and cosmochemistry. *J Petrol* 56:1607–1642. [https://doi.org/10.1016/0012-821x\(77\)90060-7](https://doi.org/10.1016/0012-821x(77)90060-7)
- Stelten ME, Cooper KM, Vazquez JA, Calvert AT, Glessner JGG (2015) Mechanisms and timescales of generating eruptible rhyolitic magmas at Yellowstone Caldera from zircon and sanidine geochronology and geochemistry. *J Petrol* 56:1607–1642. <https://doi.org/10.1093/petrology/egv047>
- Turniak K, Mazur S, Domańska-Siuda J, Szuskiewicz A (2014) SHRIMP U–Pb zircon dating for granitoids from the Strzegom–Sobótka Massif, SW Poland: Constraints on the initial time of Permo-Mesozoic lithosphere thinning beneath Central Europe. *Lithos* 208–209:415–429. <https://doi.org/10.1016/j.lithos.2014.09.031>
- Valley JW, Lackey JS, Cavoie AJ, Clechenko CC, Spicuzza MJ, Basei MAS, Bindeman IN, Ferreira VP, Sial AN, King EM, Peck WH, Sinha AK, Wei CS (2005) 4.4 billion years of crustal maturation: oxygen isotope ratios of magmatic zircon. *Contrib Miner Petrol* 150:561–580. <https://doi.org/10.1007/s00410-005-0025-8>
- van Wees J-D, Stephenson RA, Ziegler PA, Bayer U, McCann T, Dedlez R, Gaupp R, Narkiewicz M, Bitzer F, Scheck M (2000) On the origin of the Southern Permian Basin, Central Europe. *Mar Petrol Geol* 17:43–59. [https://doi.org/10.1016/S0264-8172\(99\)00052-5](https://doi.org/10.1016/S0264-8172(99)00052-5)
- Vervoort JD, Patchett PJ, Söderlund U, Baker M (2004) Isotopic composition of Yb and the determination of Lu concentrations and Lu/Hf ratios by isotope dilution using MC-ICPMS. *Geochem Geophys Geosyst*. <https://doi.org/10.1029/2004gc000721>
- Watts KE, Bindeman IN, Schmitt AK (2011) Large-volume rhyolite genesis in caldera complexes of the Snake River Plain: insights from the Kilgore Tuff of the Heise Volcanic Field, Idaho, with comparison to Yellowstone and Bruneau–Jarvis rhyolites. *J Petrol* 52:857–890. <https://doi.org/10.1093/petrology/egr005>
- Wiedenbeck M, Allé P, Corfu F, Griffin WI, Meier M, Oberli F, von Quadt A, Roddick JC, Spiegel W (1995) Three natural zircon standards for U–Th–Pb, Lu–Hf, trace element and REE analyses. *Geostand News* 19:1–23. <https://doi.org/10.1111/j.1751-908X.1995.tb00147.x>
- Wiedenbeck M, Hancher JM, Peck WH, Sylvester P, Valley J, Whitehouse M, Kronz A, Morishita Y, Nasdala L, Fiebig J, Franchi I, Girard J-P, Greenwood RC, Hinton R, Kita N, Mason PRD, Norman M, Ogasawara M, Piccoli PM, Rhede D, Satoh H, Schulz-Dobrick B, Skår O, Spicuzza MJ, Terada K, Tindle A, Togasji S, Vennemann T, Xie Q, Zheng Y-F (2004) Further characterisation of the 91500 zircon crystal. *Geostand Geoanal Res* 28:9–39. <https://doi.org/10.1111/j.1751-908X.2004.tb01041.x>
- Woodhead JD, Hergt JM (2005) A Preliminary appraisal of seven natural zircon reference materials for in situ Hf isotope determination. *Geostand Geoanal Res* 29:183–195. <https://doi.org/10.1111/j.1751-908X.2005.tb00891.x>
- Woodhead J, Hergt J, Shelley M, Eggins S, Kemp R (2004) Zircon Hf-isotope analysis with an excimer laser, depth profiling, ablation of complex geometries, and concomitant age estimation. *Chem Geol* 209:121–135. <https://doi.org/10.1016/j.chemgeo.2004.04.026>
- Zeh A, Gerdes A (2010) Baltica- and Gondwana-derived sediments in the Mid-German Crystalline Rise (Central Europe): implications for the closure of the Rheic ocean. *Gondwana Res* 17:254–263. <https://doi.org/10.1016/j.gr.2009.08.004>
- Żelaźniewicz A, Oberć-Dziedzic T, Fanning CM, Protas A, Muszyński A (2016) Late Carboniferous–early Permian events in the Trans-European Suture Zone: tectonic and acid magmatic evidence from Poland. *Tectonophysics* 675:227–243. <https://doi.org/10.1016/j.tecto.2016.02.040>
- Zielhuis A, Nolet G (1994) Deep seismic expression of an ancient plate boundary in Europe. *Science* 265:79–81. <https://doi.org/10.1126/science.265.5168.79>